Nat. Hazards Earth Syst. Sci. Discuss., doi:10.5194/nhess-2016-391, 2017
Manuscript under review for journal Nat. Hazards Earth Syst. Sci.
Published: 10 January 2017

Natural Hazards and Earth System Sciences
Discussions

Hazard Assessment Comparison of Tazhiping Landslide Before and After Treatment

Dong Huang [1]*, JianPing Qiao[1], Meng Wang[1]

1. Key Laboratory of Mountain hazards and Surface process, Institute of Mountain hazards and Environment, Chinese Academy of Science, Chengdu 610041, China
*Corresponding author (dhuang@imde.ac.cn).

Abstract: Through investigation and analysis of geological conditions and mechanical parameters of the Taziping landslide, the finite volume method was adopted, and, the rheological model was adopted to simulate the landslide and avalanche entire mass movement process. The present paper adopted the GIS platform to simulate the mass movement process before and after treatment. This paper also provided the conditions and characteristic parameters of soil deposits (thickness, speed, and stresses) during the landslide mass movement process and mapped the 3D division of hazard zones before and after landslide treatment. Results indicated that the scope of hazard zones contracted after engineering treatment of the landslide. The extent of high-hazard zones was reduced by about 2/3 of the area before treatment, and characteristic parameters of the mass movement process after treatment decreased to 1/3 of those before treatment. Despite engineering treatment, the Taziping landslide still poses significant hazard to nearby settlements. Therefore, we propose that houses located in high-hazard zones be relocated or reinforced for protection.

Keywords: finite volume method; rheological model; motion feature parameters; hazard assessment

1. Introduction

The hazards of a landslide include scope of influence (i.e., source area, possible path area, and backward and lateral expansion area) and secondary disasters (i.e., reservoir surge, blast, and landslide-induced barrier lake). A typical landslide hazard assessment aims to propose a systematic hazard assessment method with regard to a given position or a potential landslide. Current research on typical landslide hazard assessment remains immature, and there are multiple methods for interpreting landslide hazards. To be specific, the scope of influence prediction of a landslide refers to deformation and instability characteristics such as sliding distance, movement speed, and bulking thickness range. The movement behavior of a landslide mass is related to its occurrence, sliding mechanisms, mass characteristics, sliding path, and many other factors. Current landslide movement prediction methods include empirical prediction and numerical simulation.

Empirical prediction method: The empirical prediction method involves analyzing landslide flow through the collection of landslide parameters in the field. It

Nat. Hazards Earth Syst. Sci. Discuss., doi:10.5194/nhess-2016-391, 2017
Manuscript under review for journal Nat. Hazards Earth Syst. Sci.
Published: 10 January 2017

Natural Hazards and Earth System Sciences
Discussions

further consists of the geomorphologic method (Costa, 1984; Jackson *et al*., 1987; Scott *et al*., 1993), the geometric change method (Zhang *et al.*, 1994; Finlay *et al*., 1999; Michael-Leiba M *et al*., 2003), and the volume change method (Fannin *et al*., 2001). Empirical models are commonly simple and easy to apply, and the required data are easy to obtain as well. **Numerical simulation method:** Numerical simulation methods are further divided into the continuous deformation analysis method (Hungr, 1995; Evans *et al*., 2009; Zhang .Y, 2013; Wang. L, *et al.*, 2016), the discontinuous deformation analysis method (Shi.G.H, 1988; Yin *et al.*, 2002), and the simplified analytical simulation method (Christen et al., 2010a; Sassa, 2011; Bartelt *et al.*, 2012; Du *et al.*, 2015). The numerical simulation method expresses continuous physical variables using the original spatial and temporal coordinates with geometric values of discrete points. Numerical simulations follow certain rules to establish an algebraic equation set in order to obtain approximate solutions for physical variables.

Empirical prediction models only provide a simple prediction of the sliding path. Due to the differences in geological environments, empirical prediction models commonly have low generality. The continuous deformation method has the advantage of an extremely strong replication capability, but it is not recommended when analyzing landslide-debris flows, lahars, or debris flows because of complicated rheological behaviors. The fluid mechanics-based discontinuous deformation method has several shortcomings such as, great computational burden, difficult parameter selection, and difficult 3D implementation. The simplified analytical simulation method fully takes into account the flow state properties of landslides before introducing a rheological model and can easily realize 3D implementation on the GIS platform. On that account, this paper adopted the continuous fluid mechanics-based finite volume method (simplified analytical simulation method). We introduce a rheological model on the basis of using mass as well as momentum and energy conservation to describe the movement of landslides. We also employed GIS analysis to simulate the entire movement process of Taziping landslide and map the 3D division of hazard zones.

2. Methods

2.1 Kinetic analysis method

Adopting the continuous fluid mechanics-based finite volume method, this paper took into account erosion action on the lower surface of the sliding mass and the change in frictional resistance within the landslide-debris flow in order to establish a computational model. The basic idea is to divide the calculation area into a series of non-repetitive control volumes, ensuring that there is a control volume around each grid point. Each control volume is then integrated by the unresolved differential equation in order to obtain a set of discrete equations. The unknown variable is the numerical value of the dependent variable at each grid point. To solve the integral of a control volume, we make a hypothesis about the change rule of values among grid points, that is, about their piecewise distribution profile. The finite volume method can satisfactorily overcome the finite element method's weakness of slow calculation,

Nat. Hazards Earth Syst. Sci. Discuss., doi:10.5194/nhess-2016-391, 2017
Manuscript under review for journal Nat. Hazards Earth Syst. Sci.
Published: 10 January 2017

Natural Hazards and Earth System Sciences
Discussions

and solve the problem of complex region processing. Thus, we adopted the finite volume method to establish the kinematic model for the landslide flow process.

The core of the finite volume method is domain discretization. The finite volume method uses discrete points as a substitute for continuous space. The physical meaning of the discrete equation is the conservation of the dependent variable in a finite control volume. Establishment of the conservation equation is based on the continuous movement model, that is, the continuity hypothesis about landslide substances. We divided the landslide mass into a series of units and made the hypothesis that each unit has consistent kinematic parameters (speed at a depth, density, etc.) and physical parameters (Fig.1). We also established an Eulerian coordinate system-based conservation equation with regard to each control volume.

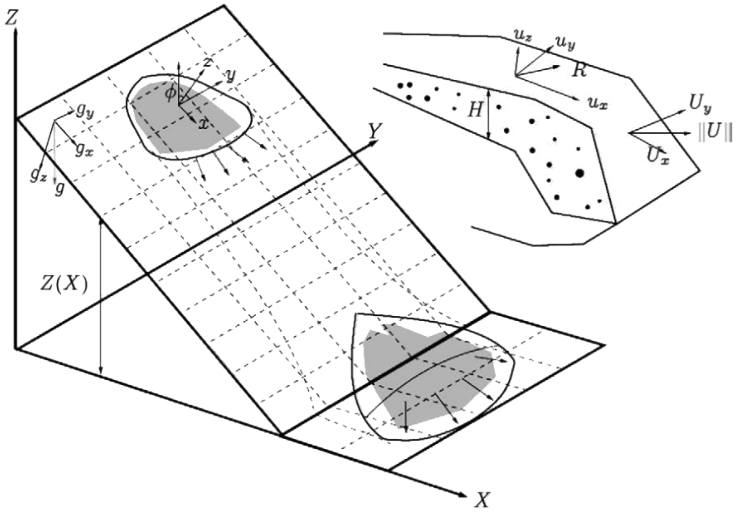

Fig.1 Schematic diagram of finite volume discretization

2.2 Control equation

The computational domain is defined as directions x and y, and the topographic elevation is given the coordinate $z(x,y)$. $H(x,y,t)$ is assumed as the change relationship of landslide thickness with time; $U_x(x,y,t)$ and $U_y(x,y,t)$ respectively represent the mean movement speeds along directions x and y at moment t; $n_x = U_x \Big/ \sqrt{U_x^2 + U_y^2}$ and $n_y = U_y \Big/ \sqrt{U_x^2 + U_y^2}$ represent the cosinoidal and sinusoidal flow vectors of the landslide on the plane x-y. The mean flow speed of substances is defined as $U = \sqrt{U_x^2 + U_y^2}$.

Nat. Hazards Earth Syst. Sci. Discuss., doi:10.5194/nhess-2016-391, 2017
Manuscript under review for journal Nat. Hazards Earth Syst. Sci.
Published: 10 January 2017

Thus, the mass balance equation becomes:

$$\partial_t H + \partial_x (HU_x) + \partial_y (HU_y) = \dot{Q} \tag{1}$$

wherein, $\dot{Q}(x,y,t)$ represents the change rate (entrainment rate) of landslide volume with time.

Assuming that $l(x,y,t)$ represents the movement distance of the landslide with time, we can obtain:

$$\dot{Q} = \begin{cases} 0 & if \quad h_i = 0 \\ \dfrac{\rho_i}{\rho_a} h_i \dfrac{U}{l} & if \quad k_i l \geq h_i \\ \dfrac{\rho_i}{\rho_a} k_i U & if \quad k_i l < h_i \end{cases} \tag{2}$$

wherein, h_i represents the thickness of the ith layer of the landslide in the movement process; ρ_i represents the density of the ith layer of the landslide in the movement process; ρ_a represents the density of the landslide; the dimensionless parameter k_i represents the entrainment rate.

The momentum balance equation is:

$$\partial_t (HU_x) + \partial_x (HU_x^2 + \frac{g_z k_{a/p} H^2}{2}) + \partial_y (HU_x U_y) = S_{gy} - S_f(R)[n_x] \tag{3}$$

$$\partial_t (HU_y) + \partial_y (HU_y^2 + \frac{g_z k_{a/p} H^2}{2}) + \partial_x (HU_x U_y) = S_{gx} - S_f(R)[n_y] \tag{4}$$

wherein, $S_{gx} = g_x H$ and $S_{gy} = g_y H$ represent the dynamic components of the acceleration of gravity in directions x and y; $g = (g_x \quad g_y \quad g_z)$ represents the vector of the acceleration of gravity; $k_{a/p}$ represents the pressure coefficient of soil; ρ_a represents the density of the landslide; the dimensionless parameter k_i represents the entrainment rate; $S_f(R)$ represents the frictional resistance.

The kinetic energy balance equation is:

$$\partial_t (HR) + \partial_x (HRU_x) + \partial_y (HRU_y) = \dot{P} - \dot{D} \tag{5}$$

wherein, $R(x,y,t)$ represents the random mean kinetic energy of the landslide;

Nat. Hazards Earth Syst. Sci. Discuss., doi:10.5194/nhess-2016-391, 2017
Manuscript under review for journal Nat. Hazards Earth Syst. Sci.
Published: 10 January 2017

Natural Hazards and Earth System Sciences
Discussions

$\dot{P}(x,y,t)$ and $\dot{D}(x,y,t)$ represent the random increased kinetic energy and decreased kinetic energy of the landslide.

2.3 Constitutive relationship

The improved Voellmy rheological model is applied in the computational simulation of the landslide. See the computational formula below:

$$S_f = \frac{u_i}{\|U\|}\left(h\mu g_z + R_t U^2 + R_\zeta U^2\right) \tag{6}$$

$$R_t = \mu h \frac{U^T K U}{U^2}, R_\zeta = \frac{g}{\zeta} \tag{7}$$

wherein, $u_i/\|U\|$ represents the unit vector in the movement direction of the landslide; μ represents the Coulomb friction coefficient, and is related to $R(x,y,t)$, the random mean kinetic energy of the landslide; R_t represents the gravity-related frictional force coefficient; K represents the substrate surface curvature; ζ represents the viscous friction coefficient of the "turbulent flow".

2.4 HLLE-Heun numerical solution

Synthesizing control equations (1), (3), (4) and (5), we can obtain the simplified form of the nonlinear hyperbola equation:

$$\partial_t V + \nabla \cdot F(V) = G(V) \tag{8}$$

$$V = \begin{pmatrix} H \\ HU_x \\ HU_y \\ HR \end{pmatrix} \qquad G(V) := \begin{pmatrix} \dot{Q} \\ S_{gx} - S_{fx} \\ S_{gy} - S_{fy} \\ \dot{P} - \dot{D} \end{pmatrix}$$

$$F(V) = \begin{pmatrix} HU_x & HU_y \\ HU_x^2 + g_z k_{a/p}\frac{H^2}{2} & HU_x U_y \\ HU_x U_y & HU_y^2 + g_z k_{a/p}\frac{H^2}{2} \\ HRU_x & HRU_y \end{pmatrix}$$

wherein, $V(x,y,t)$ represents a vector equation consisting of four unknown vector variables; $F(V)$ represents the flux function; $G(V)$ represents the source term. Based on the HLLE equation of the finite volume method and the quadrilateral grid, the node layout can adopt the grid center pattern, and the normal flux along one side of the control volume can be represented by the flux at the center of the side. The finite volume discretization adopting the control volume as unit is depicted in Fig.1; the

Nat. Hazards Earth Syst. Sci. Discuss., doi:10.5194/nhess-2016-391, 2017
Manuscript under review for journal Nat. Hazards Earth Syst. Sci.
Published: 10 January 2017

Gauss theorem can be followed for the integration of equation (8), wherein C_i represents the unit volume; after converting the volume integral flux function $F(V)$ into the curved surface integral, we can obtain:

$$\int_{C_i} \partial_t V dx + \oint_{\partial C_i} F(V) \cdot n_i d\sigma = \int_{C_i} G(V) dx \tag{9}$$

wherein, n_i represents the outward normal direction vertical to unit C_i at the boundary; through adopting the HLL format for the discretization of surface integral, the following simplified form can be obtained:

$$V_i^{(*)} = V_i^{(n)} + \frac{\Delta t}{A_{C_i}} \Delta F_i^{(HLL)} \left(V^{(n)} \right) \tag{10}$$

$$V_i^{(**)} = V_i^{(*)} + \frac{\Delta t}{A_{C_i}} \Delta F_i^{(HLL)} \left(V^{(*)} \right) \tag{11}$$

$$V_i^{(n+1)} = \frac{1}{2} \left(V_i^{(n)} + V_i^{(**)} \right) \tag{12}$$

wherein, $V_i^{(n)}$ represents the mean value of unit variables at moment $t^{(n)}$; $V^{(n)}$ represents the mean value of the entire grid at moment $t^{(n)}$; $\Delta t := t^{(n-1)} - t^{(n)}$ represents the calculated time step; A_{C_i} represents the area of unit C_i; $\Delta F_i^{(HLL)}$ represents the approximate value of the curved surface integral, as shown below:

$$\Delta F_i^{(HLL)} \left(V^{(n)} \right) := -\sum_{j=1}^{4} F_{ij}^{(HLL)} \left(V^{(n)} \right) n_{ij} \Delta X \tag{13}$$

wherein, n_{ij} represents the outward normal direction of the i th unit at boundary j; the flux calculation term $F_{ij}^{(HLL)} \left(V^{(n)} \right)$ represents the approximate solution mode of the Riemann problem of the i th unit at boundary j; see the computational formula below:

$$F_{ij}^{(HLL)} \left(V^{(n)} \right) = \begin{cases} F\left(V_L^{(n)} \right) & 0 \le S_L \\ \dfrac{S_R F\left(V_L^{(n)} \right) - S_L F\left(V_R^{(n)} \right) + S_R S_L F\left(V_R^{(n)} - V_L^{(n)} \right)}{S_R - S_L} & S_L \le 0 \le S_R \\ F\left(V_R^{(n)} \right) & S_R \le 0 \end{cases} \tag{14}$$

wherein, $V_L^{(n)}$ and $V_R^{(n)}$ respectively represent the approximate values of $V^{(n)}$ on both sides of boundary j of the i th unit; S_L and S_R respectively represent the wave

Nat. Hazards Earth Syst. Sci. Discuss., doi:10.5194/nhess-2016-391, 2017
Manuscript under review for journal Nat. Hazards Earth Syst. Sci.
Published: 10 January 2017

speeds on the left and right sides. Refer to the computational method described by Toro (1992). In addition, the gradient magnitude in the original second-order difference equation can be limited through multiplication with the flux limiter, and the second-order format of the TVD property can be constructed to avoid the occurrence of numerical oscillation. Refer to the specific method described by LeVeque (2002).

In this paper numerical solver used within RAMMS, which was specifically designed to provide landslide(avalanche) engineers with a tool that can be applied to analyze problems that two-dimensional depth-averaged mass and momentum equations on three-dimensional terrain using both first and second-order finite volume methods (Christen et al., 2010b).

3. Study area and data

3.1 Taziping landslide

Taziping landslide is located in the southeast of the Hongse Village, Hongkou Town, Dujiangyan City of Sichuan Province. The site is located at (E103°37′46″, N31°6′29″), 68 km away from Chengdu City to the east and 20 km away from the Dujiangyan Urban District (Fig. 2). Its geomorphic unit is a middle-mountain tectonic erosion area, falling within the slope geomorphology on the right bank of the Baisha River Valley. As an colluvial layer landslide triggered by the Wenchuan Earthquake, Taziping Landslide is a large-scale landslide as shown in Fig. 3. It has a gradient of 25°-40° with an average of about 32°. The landslide has an apparent round-backed armchair contour, and has formed a steep main scarp, which has a gradient of 35°-50° and an elevation of about 1,370 m. The toe is located on the south side of the mountain road, and has an elevation of about 1,007 m. The landslide has an elevation difference of about 363 m, and the main sliding direction of 124°NE. The landslide mass is in an irregular semi-elliptical shape, and has a length of about 530 m, an average width of 145 m and a landslide area of approximately 7.68×10^4 m^2. The landslide mass is gravelly soil in lithology, and is covered on the surface by silty clay mingled with gravels. In terms of spatial distribution, it is thick in the middle and thin on the lateral edges, and has a thickness of 20-25 m and a volume of approximately 1.16×10^6 m^3. During the earthquake, the landslide mass slid to cover the northern mountain slope mass of the Hongse Village Miaoba settlement. The landslide has an apparent front edge boundary, and there is also a swelling deformation.

Nat. Hazards Earth Syst. Sci. Discuss., doi:10.5194/nhess-2016-391, 2017
Manuscript under review for journal Nat. Hazards Earth Syst. Sci.
Published: 10 January 2017

Natural Hazards and Earth System Sciences
Discussions

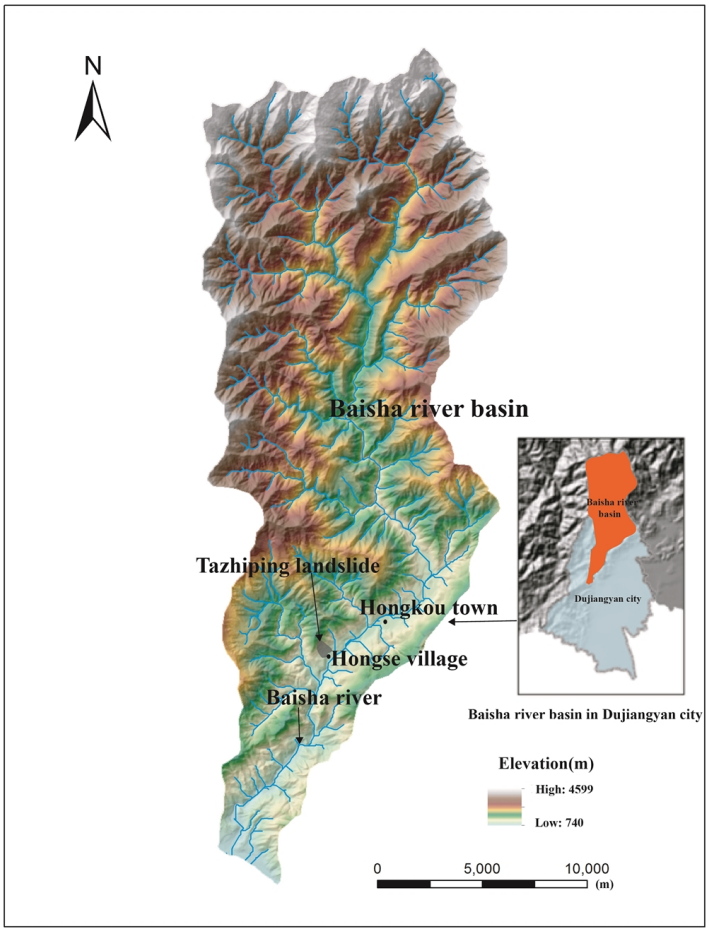

Fig.2 Location of Tazhiping landslide, Baisha river basin, Dujiangyan city (the landslide triggered by Wenchuan Ms 8.0 earthquake on May 12, 2008)

Nat. Hazards Earth Syst. Sci. Discuss., doi:10.5194/nhess-2016-391, 2017
Manuscript under review for journal Nat. Hazards Earth Syst. Sci.
Published: 10 January 2017

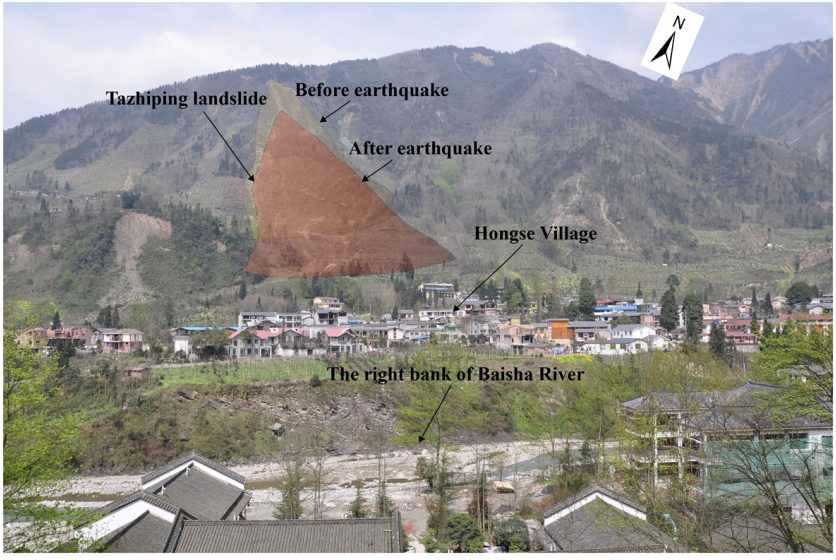

Fig.3 Taziping Landslide

After Wenchuan Earthquake, the massive colluvial deposits covers on the mountain slope, and the landslide mass is dominated by the colluvium. The colluvium is mainly distributed on the top surface of the landslide mass in the thickness of 0.5-5.0 m, and is mainly constituted by rubbles and gravels. The mass consists of a small amount of fine gravel substances which are gray or grayish-green, and dominated by andesite in composition, generally with a block size of 20-150 cm. Field survey indicates that the rubbles in the surface layer have a maximum diameter exceeding 2 m, and that fine gravel substances are filled among rubbles in a loose structure. Within the thickness of 5-10 m, the landslide mass is constituted of a small amount of yellowish-brown and gray-brown silty clay mingled with 5-40% of non-uniformly distributed broken rubbles. Within the thickness of 10-25 m, there is a wide distribution of gravelly soil. The soil is grayish-green or variegated in color, is slightly compact and non-uniform, and has a broken stone content of about 50%. The parent rock of the broken stones is andesite, filled with silty clay or silt (Fig.4). Table 1 shows the parameters of the surface gravelly soil of the landslide mass based on the field sampling.

Tab.1 Parameters of the surface soil of Taziping Landslide

Internal friction angle (°)		Cohesion (kPa)	Relative compactness	Natural void ratio	Dry density (kN·m-3)	Specific gravity (g·cm-3)
Peak	Residual					
27.5	23	20.5	53%	0.789	15.357	2.492

Nat. Hazards Earth Syst. Sci. Discuss., doi:10.5194/nhess-2016-391, 2017
Manuscript under review for journal Nat. Hazards Earth Syst. Sci.
Published: 10 January 2017

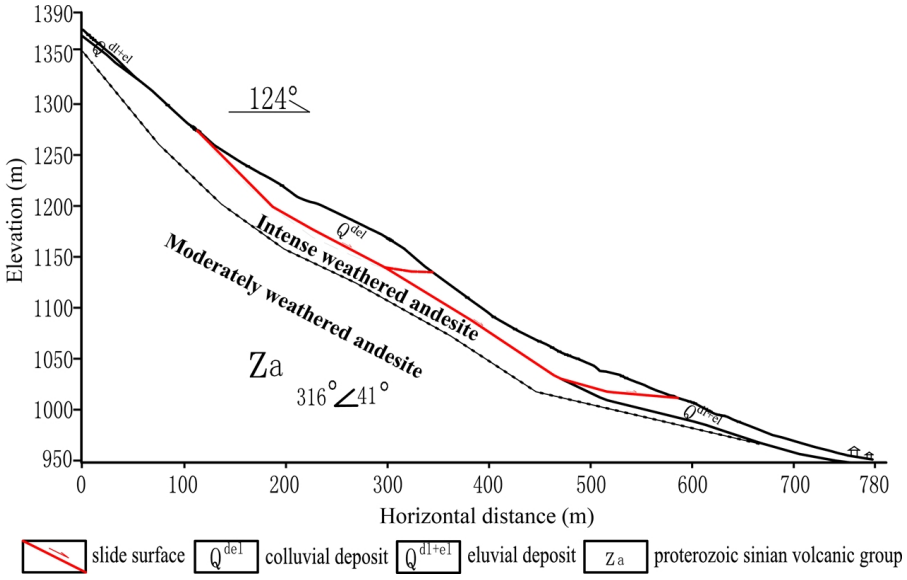

Fig.4 Geological profile of Taziping Landslide

The landslide is an unconsolidated mass containing relatively large amounts of crushed stones and silty clay (Fig.5). Its loose structure and strong permeability facilitate infiltration of surface water. The Wenchuan earthquake aggravated the deformation of the landslide making deposits more unconsolidated, further reducing the stability of the landslide mass. During persistent rainfall, surface water infiltrates the landslide slope resulting in increased water pressure within the landslide mass and reduced shear strength on the sliding surface. Thus, rainfall constitutes the primary inducing factor of the upper Taziping landslide. After infiltrating the loose layer, water saturates the slope increasing the dead weight of the sliding mass and reducing the shear strength of soil in the sliding zone. Infiltration into the landslide mass also increases the infiltration pressure of perched water, drives deformation, and poses a great threat to villages located at the front of the landslide. Slide-resistant piles and backfill were place at the toe of the slope in order to reduce the hazards of future slides. The slide-resistant piles have enhanced the overall stability of the slope, however, under heavy rainfall the upper unconsolidated landslide deposits may cut out from the top of the slide-resistant piles.

Nat. Hazards Earth Syst. Sci. Discuss., doi:10.5194/nhess-2016-391, 2017
Manuscript under review for journal Nat. Hazards Earth Syst. Sci.
Published: 10 January 2017

Natural Hazards and Earth System Sciences
Discussions

(a) Material on the landslide surface (b) Material in the shear zone

Fig.5 Colluvial deposits covers on the mountain slope

Therefore we simulate possible movement states of the Taziping landslide before and after treatment with slide-resistant piles, comparatively analyzed the kinetic parameters in the movement process, and mapped the 3D division of hazard zones.

3.2 Hazard prediction before treatment

It was assumed that the landslide was damaged before engineering treatment. According to field investigation, the sliding mass had an estimated starting volume of about 600,000m^3 and a mean thickness of 8m. Based on the survey report and field investigation (Hydrologic Engineering and Geological Survey Institute of Hebei Province, 2010), we adopted the survey parameters of Tab.2 for the simulated calculation.

Tab.2 Model calculation parameters

Unit weight $\gamma(kN \cdot m^{-3})$	**Coulomb model coefficient** u	**Viscous friction coefficient** $\zeta(m \cdot s^{-2})$	**Erosional entrainment rate** k_i
20.8	0.45	500	0.0001

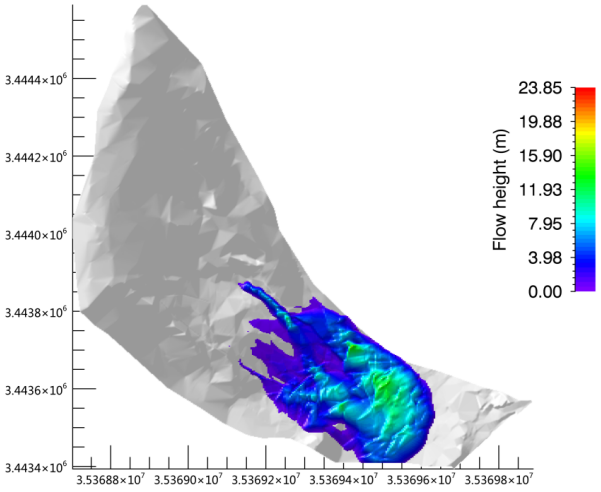

(a) Thickness

Nat. Hazards Earth Syst. Sci. Discuss., doi:10.5194/nhess-2016-391, 2017
Manuscript under review for journal Nat. Hazards Earth Syst. Sci.
Published: 10 January 2017

Natural Hazards and Earth System Sciences
Discussions
Open Access
EGU

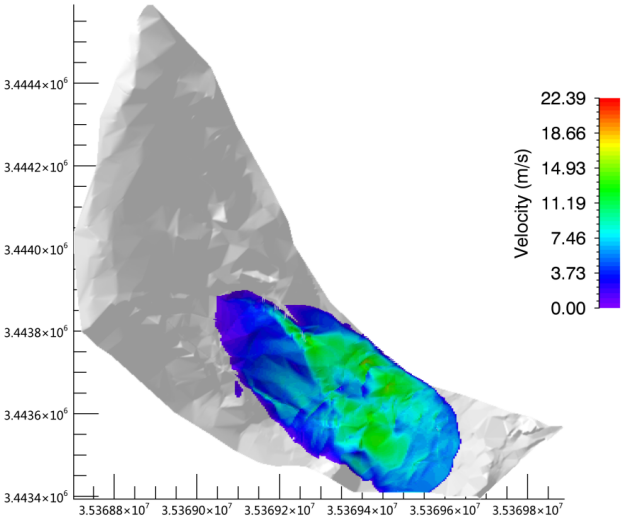

(b) Speed

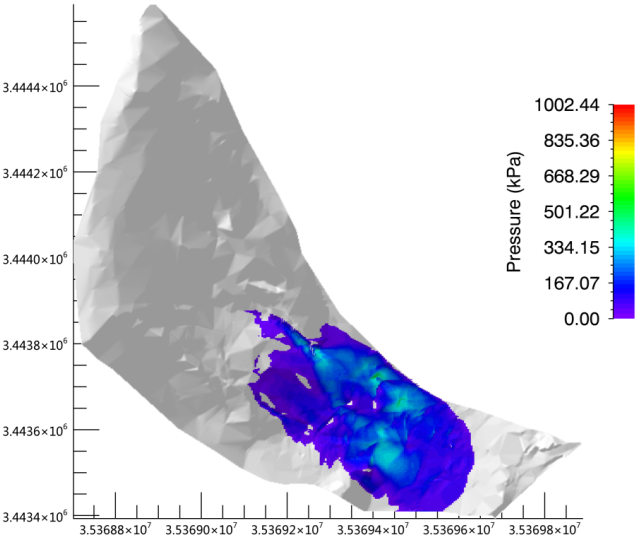

(c) Pressure

Fig.6 Movement characteristic parameters of Taziping landslide (before treatment)

See the kinematic characteristic parameters of the landslide deposits in Fig.6. As shown by the calculation results, ① deposits accumulated during the landslide movement process had a maximum thickness of 23.85m, located around the surface gully of the middle and upper slope. The middle and lower deposits had a thickness of about 5-10m; ② the middle and lower movement speed of the landslide ranged from

Nat. Hazards Earth Syst. Sci. Discuss., doi:10.5194/nhess-2016-391, 2017
Manuscript under review for journal Nat. Hazards Earth Syst. Sci.
Published: 10 January 2017

Natural Hazards and Earth System Sciences
Discussions

278 3m/s and 7m/s; ③ the landslide had a mean pressure of about 500kPa, and the
279 pressure of the middle and lower deposits was about 200kPa. Thus, three-story and
280 lower houses within the deposition range might be buried, and it was further
281 suggested that the design strength of the gable walls of houses on the middle and
282 upper parts of the deposit be increased above 300kPa.
283
284 **3.3 Hazard prediction after treatment**
285 After fully accounting for the slide-resistant piles and mounds, we introduced the
286 Morgenstern-Price method (Morgenstern et al., 1965) to calculate the stability
287 coefficient of Taziping landslide after treatment. The physico-mechanical parameters
288 under a saturated state (Hydrologic Engineering and Geological Survey Institute of
289 Hebei Province, 2010) were adopted to search for the sliding plane of the landslide.
290 Under rainfall conditions, the middle area of Taziping landslide was unstable. Loose
291 deposits in the middle part of the landslide might convert into high-water landslide
292 substances and cut out from the top of the slide-resistant piles. In the damaged area,
293 the slope had a rear edge wall elevation of about 1,170m. Its front edge was located
294 on the south side of the mountain road, with an elevation of about 1,070m and a
295 length of about 180m. Thus, the scale of the rainfall-damaged is estimated to be about
296 250,000m^3, with a mean thickness of about 6m. The parameters in Tab.2 were again
297 adopted for the simulated calculation.

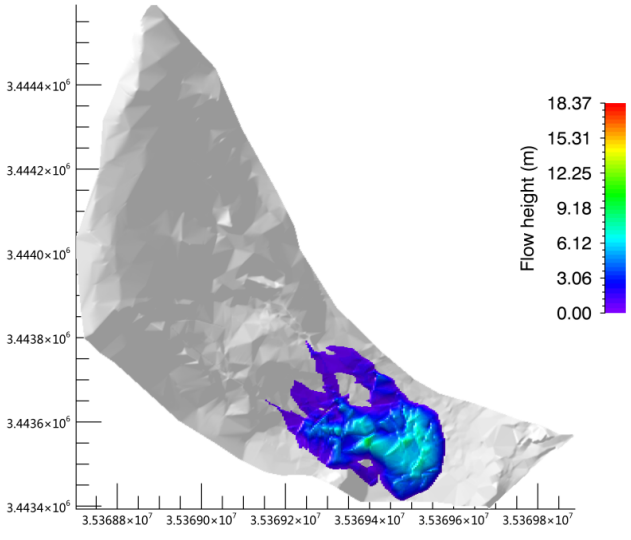

298
299 (a) Thickness

Nat. Hazards Earth Syst. Sci. Discuss., doi:10.5194/nhess-2016-391, 2017
Manuscript under review for journal Nat. Hazards Earth Syst. Sci.
Published: 10 January 2017

Natural Hazards and Earth System Sciences
Discussions
Open Access
EGU

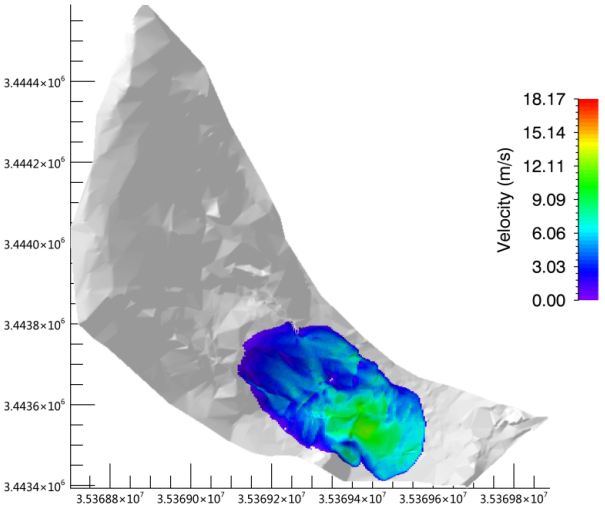

(b) Speed

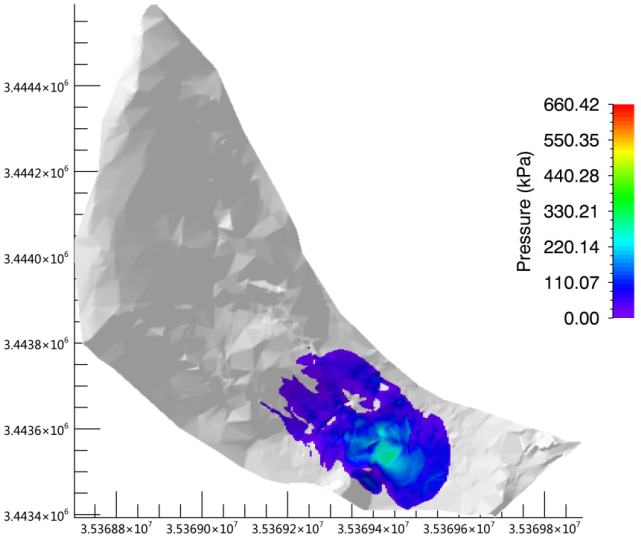

(c) Pressure

Fig.7 Movement characteristic parameters of Taziping landslide (after treatment)

Provided in Fig.4 are the kinematic characteristics of the landslide deposit. ① Deposits accumulated during the landslide movement process had a maximum thickness of 18.37m, located around the surface gully of the middle and upper slope. Middle and lower deposits had a thickness of approximately 3-5m. ② The middle and lower movement speed of the landslide deposits ranged between 3m/s and 5m/s. ③ The landslide had a mean pressure of about 330kPa, and the pressure of the middle

Nat. Hazards Earth Syst. Sci. Discuss., doi:10.5194/nhess-2016-391, 2017
Manuscript under review for journal Nat. Hazards Earth Syst. Sci.
Published: 10 January 2017

and lower deposits was about 100kPa. Thus, it could be held that two-story and lower houses within the deposition range might be buried. It was further suggested that the design strength of the gable walls of houses on the middle and upper parts of the deposits be increased above 150kPa.

After treatment, the accumulation thickness and pressure of the deposits were reduced by about 1/2, and the kinematic speed was reduced by about 1/3. However, the Miaoba residential area of Red Village was still partially at hazard.

4 Results

During landslide movement, the spatial scale indexes of a landslide mass include area, volume, and thickness. The maximum thickness of the landslide is one of the direct factors influencing the building's deformation failure status. A large landslide displacement may lead to burial, collapse, or deformation failure of the building, and thus influence its safety and stability. Thus, landslide thickness constitutes an important index for assessing the hazards of a landslide disaster, and for influencing the consequences faced by disaster-affected bodies. Provided in Tab.3 is a landslide thickness-based division of the predicted hazard zones of Taziping landslide, in which the thickness of the landslide mass correlates with the ability of a building to withstand a landslide disaster. After treatment with slide-resistant piles, the hazard of a future slide was reduced by about 1/3 overall and by 2/3 in high-hazard zones.

Tab.3 Division table of the predicted hazards of Taziping landslide (unit: m^2)

Hazard zone level	Assessment index	Building damage probability	Area before treatment	Area after treatment	Increased/decreased area	Building damage characteristics
Low-hazard zone (I)	$h \leq 0.5$m	20%	44，600	38，748	-5,852	One-story houses may be damaged; houses on the landslide mass are partially damaged.
Relatively low-hazard zone (II)	0.5 m < $h \leq 1$m	50~20%	24，900	26，400	+1,500	One-story houses have a very high probability of being washed away; one-story houses on the

Nat. Hazards Earth Syst. Sci. Discuss., doi:10.5194/nhess-2016-391, 2017
Manuscript under review for journal Nat. Hazards Earth Syst. Sci.
Published: 10 January 2017

Natural Hazards and Earth System Sciences
Discussions

						landslide mass are completely damaged.
Moderate-hazard zone (III)	1m < h≤3m	80~50%	21，980	15，856	-6,124	One-story to three-story houses have a very high probability of being washed away; houses less than three stories on the landslide mass are completely damaged.
Relatively high-hazard zone (IV)	3m < h≤5m	100~80%	30，820	19，636	-11,184	One-story houses may be buried, and two-story to six-story houses have a very high probability of being washed away; houses on the landslide mass are completely damaged.
High-hazard zone (V)	h≥5m	100%	47，240	13，052	-34,188	Two-story and lower houses may be buried, and three-story and higher houses have a very

Nat. Hazards Earth Syst. Sci. Discuss., doi:10.5194/nhess-2016-391, 2017
Manuscript under review for journal Nat. Hazards Earth Syst. Sci.
Published: 10 January 2017

Natural Hazards and Earth System Sciences
Discussions
Open Access
EGU

						high probability of being washed away; houses on the landslide mass are completely damaged.
Total area:	—	—	169，540	113，700	-54,340	—

Given in Fig.8 are the 3D divisions of hazard zones of Taziping landslide before and after engineering treatment. The scope of the hazard zones changed before and after engineering treatment, particularly in the high-hazard zones. Before treatment with slide-resistant piles, the landslide posed a great hazard to eight houses on the left side of the upper Miaoba residential area. After treatment, the number of effected houses was reduced to four.

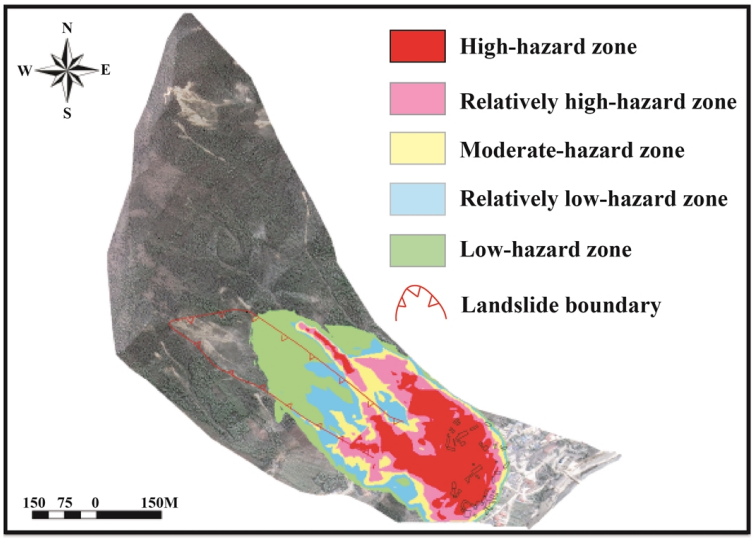

(a) Before treatment

Nat. Hazards Earth Syst. Sci. Discuss., doi:10.5194/nhess-2016-391, 2017
Manuscript under review for journal Nat. Hazards Earth Syst. Sci.
Published: 10 January 2017

Natural Hazards and Earth System Sciences
Discussions

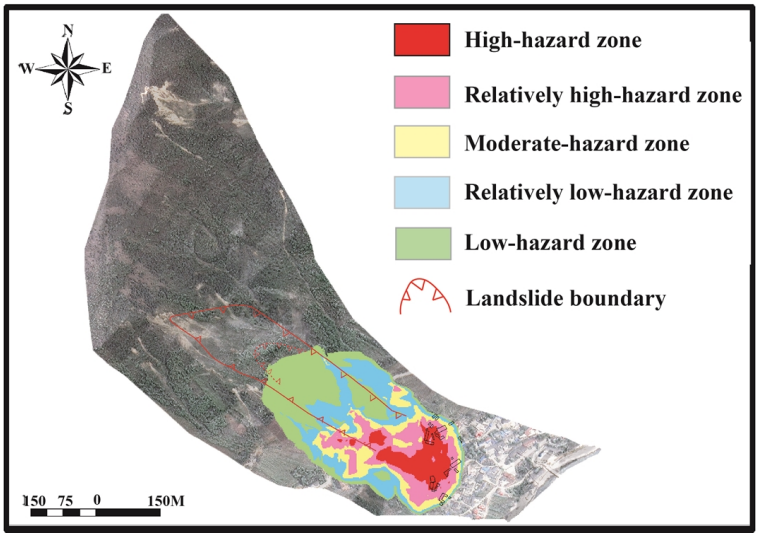

(c) After treatment

Fig.8 3D division comparison of the hazards of Taziping landslide

5 Conclusions and Discussion

Based on the finite volume method, the simulation results of Taziping landslide were consistent with the sliding path predicted by the field investigation. This correlation indicates that numerical simulation is an effective method for studying the movement processes of landslide-debris flows. The accumulation thickness and pressure of landslide deposits were reduced by about 1/2, and the kinematic speed was reduced by about 1/3 after treatment. However, the Miaoba residential area of Red Village is still partially at hazard. Considering that two-story and lower houses within the deposition range might be buried, it was further suggested that the design strength of the gable walls of houses on the middle and upper parts of the deposit be increased above 150kPa.

By utilizing a GIS platform in combination with landslide hazard assessment indexes, we mapped the 3D division of the Taziping landslide hazard zones before and after engineering treatment. The results indicated that overall hazard zones contracted after engineering treatment and, the area of high-hazard zones was reduced by about 2/3. After engineering treatment, the number of at hazard houses on the left side of the upper Miaoba residential area, was reduced from eight to four. It was thus clear that some zones are still at high hazard despite engineering treatment. Therefore, it was proposed that houses located in high-hazard zones be relocated or reinforced for protection.

Nat. Hazards Earth Syst. Sci. Discuss., doi:10.5194/nhess-2016-391, 2017
Manuscript under review for journal Nat. Hazards Earth Syst. Sci.
Published: 10 January 2017

Natural Hazards and Earth System Sciences
Discussions

Acknowledgments

This work was supported by National Natural Science Foundation of China (Grant No. 41301009) and the Hundred Young Talents Program of IMHE (SDSQB-2016-01), the International Cooperation Program of the Ministry of Science and Technology of China (Grant No.2013DFA21720). The authors express their deepest gratitude to those aids and assistances.

Reference

Bartelt, P.; Bühler, Y.; Buser, O.; Christen, M. and Meier, L. Modeling massdependent flow regime transitions to predict the stopping and depositional behavior of snow avalanches, J. Geophys. Res., 2012 .117, F01015, doi:10.1029/2010JF001957

Costa,J.E., 1984.Physical geomorphology of debris flows. Developments and Applications of Geomorphology[J]. Springer Press, 268-317.

Christen, M. Kowalski, J. and Bartelt, P. RAMMS: Numerical simulation of dense snow avalanches in three-dimensional terrain, Cold Regions Science and Technology[J]. 2010: 63, 1 - 14

Christen, M., Bartelt, P., Kowalski, J., Back calculation of the In den Arelen avalanche with RAMMS: interpretation of model results[J]. Annals of Glaciology. 2010,51(54), 161–168.

Du,J.,Yin,K.L.,Wang,J.J.,2015.Simulation of three-dimensional movement of landslide-debris flow based on finite volume method[J]. Chinese Journal of Rock Mechanics and Engineering, 34 (3): 480-488. (in Chinese)

Evans,S.G., Tutubalina,O.V., Drobyshev,V.N., et al., 2009. Catastrophic detachment and high-velocity long-runout flow of Kolka Glacier, Caucasus Mountains, Russia in 2002[J]. Geomorphology, 105: 314-321.

Fannin,R.J.,Wise,M. P.,2001. An empirical-statistical model for debris flow travel distance[J]. Canadian Geotechnical Journal, 38 (5): 982-994.

Finlay,P.J.,Mostyn,G.R.,Fell,R.,1999.Landslide risk assessment: prediction of travel distance[J]. Canadian Geotechnical Journal, 36: 556-562.

Hebei Province Institute of Hydrogeological and Engineering. 2010. Geological Investigation Engineering supplemental survey report of Hongse Village Taziping landslide in Hongkou Town of Dujiangyan City, Sichuan Province[D]. (in Chinese)

Hungr,O.A.,1995.Model for the runout analysis of rapid flow slides, debris flows and avalanches[J]. Canadian Geotechnical Journal, 32: 610-623.

Jackson, L.E., Kostashuk, R.A., MacDonald, G.M., 1987. Identification of debris flow hazard on alluvial fans in the Canadian Rocky mountains[J]. Geological Society of America, 7:155-124.

LeVeque,R., 2002. Finite Volume Methods for Hyperbolic Problems[M]. Cambridge Texts in Applied Mathematics Cambridge University Press.

Michael,L.M., 2003. Baynes F, Scott G, Granger K Regional landsliderisk to the Cairns community[J]. NatHazards, 2003,30 (2):233–249.

Morgenstern,N.R.,Price,V.E., 1965.The analysis of the stability of general slip surfaces[J].

Nat. Hazards Earth Syst. Sci. Discuss., doi:10.5194/nhess-2016-391, 2017
Manuscript under review for journal Nat. Hazards Earth Syst. Sci.
Published: 10 January 2017

414 Geotechnique, 15 (1): 79-93.
415 Sassa,K.,2011. Landslide dynamic-risk assessment technology of rain and earthquake induced
416 rapid landsildes[D]. ICL-CGS Seminar on Geo-hazards in Xi'an.
417 Scott,K.M., Vallance,J.W., 1993. History of Landslides and Debris Flows at Mount Rainier: Water
418 Fact Sheet[D]. USGS Open-File Report: 93-111.
419 Shi,G.H., 1988. Discontinuous deformation analysis - a new numerical model for the statics and
420 dynamics of block system[D]. Berkeley: University of California.
421 Wang,L.,Li,B.，Gao,Y.，et al.,2016. Run-out prediction of large thick-bedded unstable rock: A
422 case study of Daxiang unstable rock in Yangjiao town, Wulong county, Chongqing[J]. Earth
423 Science Frontiers, 23 (2):251-259. (in Chinese)
424 Yin,K.L.,Jiang,Q.H.,Wang,Y.,2002. Simulation of Landslide Movement Process by Discontinuous
425 Deformation Analysis[J]. Earth Science-Journal of China University of Geosciences,
426 27（5）: 632-636. (in Chinese)
427 Zhang,Y.J.,2013.Study on dynamic characteristics of typic rock avalanche on canyon area.
428 Shanghai Jiao Tong University[D]. (in Chinese)
429 Zhang,Z.Y., Wang,S.T., Wang,L.S.，et al., 1993. Principles of engineering
430 geology[M].Beijing：Geology Press，212-224.(in Chinese)
431